Time-Domain Measurement of Current-Induced Spin Wave Dynamics

Koji Sekiguchi,[1] Keisuke Yamada,[1] Soo-Man Seo,[2] Kyung-Jin Lee,[2] Daichi Chiba,[1] Kensuke Kobayashi,[1] and Teruo Ono[1]

[1]*Institute for Chemical Research, Kyoto University, Uji 611-0011, Japan*

[2]*Department of Materials Science and Engineering, Korea University, Seoul 136-701, Korea*

(Received 31 August 2011; published 5 January 2012)

The performance of spintronic devices critically depends on three material parameters, namely, the spin polarization in the current (P), the intrinsic Gilbert damping (α), and the coefficient of the nonadiabatic spin transfer torque (β). However, there has been no method to determine these crucial material parameters in a self-contained manner. Here we show that P, α, and β can be simultaneously determined by performing a single series of time-domain measurements of current-induced spin wave dynamics in a ferromagnetic film.

DOI: 10.1103/PhysRevLett.108.017203 PACS numbers: 75.30.Ds, 85.70.−w, 85.75.−d

The stream of electron spins can transfer spin-angular momentum to the local magnetization in a noncollinear spin structure. This spin transfer torque (STT) effect provides us an opportunity to perform all-electrical manipulation of the magnetization, which constitutes a key technology to develop spintronic devices [1–10]. While the current-induced motion of a magnetic domain wall (DW) has been focused on this issue [11–15], the STT-induced dynamics of the spin wave (SW) [16–18] is recently invoking a great interest. An advantage of this approach lies in that the SW propagation is less sensitive to uncontrollable local defects or edge roughness inherent in devices than the DW one, enabling one to capture the intrinsic nature of STT in a more transparent way. The pioneering work to relate the SW dynamics to STT was carried out in the frequency domain measurement to observe the current-induced SW Doppler frequency shift [17,18]. However, a real-time detection of this phenomenon is left unaddressed. Such an experiment is not just a complementary version of the frequency domain one but would provide further information on the nonadiabatic STT (so-called β term, which is the ratio of nonadiabatic STT to adiabatic STT) [19], whose value is still controversial but is a necessary ingredient to build up a microscopic theory and to construct reliable spintronic applications [6,19,20].

Here we report the real-time measurement of the STT-induced SW Doppler shift in a ferromagnetic film. We show that the spin polarization in the current (P) and the intrinsic Gilbert damping (α) as well as β can be simultaneously determined by performing a single series of time-domain measurements. Our scheme to derive these three parameters to govern the physics of STT relies on the following relations: The adiabaticity of STT to determine P is detected as the Doppler variation of a SW group velocity v that depends on the dc electric current j flowing in the film [see Fig. 1(a)]

$$\Delta v_{\mathrm{STT}} = u_0, \tag{1}$$

where $u_0 (= -\mu_B j P / e M_S)$ is the magnitude of adiabatic STT, P is the spin polarization, μ_B is the Bohr magneton, j is the current density, e is the electron charge, and M_s is the saturation magnetization.

The distance-dependent propagation of the magnetostatic surface mode SW gives the intrinsic damping constant α:

$$\alpha = \frac{\gamma (2\pi M_S)^2 d \exp(-2kd)}{(H_i + 2\pi M_S)\omega_0 \Lambda}, \tag{2}$$

where γ, d, k, H_i, ω_0, and Λ are the gyromagnetic ratio, a film thickness, a wave vector of the SW, an external field (y axis), the SW resonant frequency, and the SW attenuation length, respectively (Ref. [21]). Finally, the

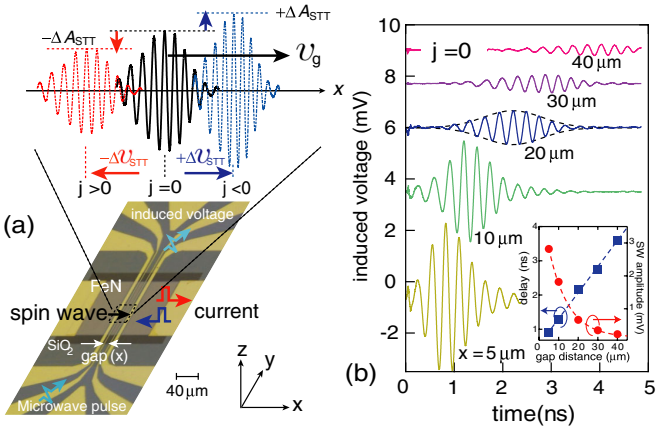

FIG. 1 (color online). The principle of the current-induced spin wave dynamics. (a) The spin wave generated by a microwave pulse is subject to a stream of STT introduced by an electric current j, resulting in the variations of both group velocity v_g and amplitude A. Upstream and downstream spin waves change their velocities into $v_g - \Delta v_{\mathrm{STT}}$ and $v_g + \Delta v_{\mathrm{STT}}$, respectively, and their amplitudes into $A - \Delta A_{\mathrm{STT}}$ and $A + \Delta A_{\mathrm{STT}}$, respectively. (b) Electric signals of the spin wave for different gap distances x, demonstrating the propagation of spin wave packets.

nonadiabaticity of STT for β in this mode is detected as a variation of the SW amplitude A induced by j:

$$\beta = -\frac{\alpha(\omega_0 - u_0 k)(\omega/-k)}{(2\pi\gamma M_S)^2 d\exp(-2kd)} + \frac{(\omega_0 - u_0 k)u_0 + (2\pi\gamma M_S)^2 d\exp(-2kd)}{\gamma(H_i + 2\pi M_S)u_0 k}\frac{\ln(\tilde{A}_{\mathrm{STT}})}{x}, \quad (3)$$

where x, k, and d are the propagating distance of the SW, the wave vector of the SW, and the film thickness, respectively. $\tilde{A}_{\mathrm{STT}}$ is a normalized SW amplitude given by $\tilde{A}_{\mathrm{STT}} = A(u_0 \neq 0)/A(u_0 = 0)$ (Ref. [21]). Interestingly, the first term on the right-hand side of Eq. (3) is independent of the SW amplitude. This indicates that there is the nonzero $\Delta A[\equiv A(u_0 \neq 0) - A(u_0 = 0)]$ in the adiabatic limit ($\beta = 0$). Note that in the time-domain measurement, the time delay is different depending on the adiabatic STT (Doppler shift). Since the damping is related to the energy dissipation rate, a longer time delay corresponds to more attenuation of the SW amplitude. Thus, there is a β-independent SW attenuation, corresponding to the first term of Eq. (3).

The microfabricated device in our time-resolved propagating spin wave spectroscopy [22] is a Permalloy film ($Fe_{19}Ni_{81}/SiO_2$, thickness: 35/35 nm), which has a pair of metal electrodes as a source and drain of the spin-polarized current to affect the SW propagation. To minimize the effect of Joule heating, we applied a pulse current. External magnetic fields (= 10 mT) magnetize the wire in the y-axis direction so that the SWs can propagate as a magnetostatic surface wave (MSSW) [23,24]. SWs are excited and detected with a pair of asymmetric coplanar strip (ACPS) transmission lines over the film [25]. For the time-resolved measurement of current-induced SW dynamics, we launched voltage pulses into one ACPS with 65-ps rise times in 100 kHz repetition frequency, causing a microwave magnetic field to generate a SW. The SW propagates in both directions normal to the ACPS and induces an additional magnetic flux on the other ACPS connected to a 20 GHz sampling oscilloscope or 8 GHz real-time oscilloscope. The present study is performed by measuring a set of devices where the gap distance (x) between the ACPSs varies from 5 to 40 μm.

Figure 1(b) presents the detected SW signal in the absence of electric current ($j = 0$). As shown in the inset in Fig. 1(b), the SW is characterized by the envelopes of packets, and the group velocity is determined to be $v_g = 13.1$ km/s from the observed gap-dependent delay. Furthermore, the gap-dependent decay of the SW amplitude allows us to determine the attenuation length $\Lambda = 15$ μm, which directly gives the intrinsic Gilbert damping $\alpha = 0.0082$ by Eq. (2). Note that the resonant frequency and wave vector of the SW were deduced by the Fourier analysis of time-domain waveform and by ACPS geometry, respectively [25].

The current-induced SW dynamics are evaluated by the background subtraction: $\Delta v_{\mathrm{STT}} = [\Delta v_g(k) - \Delta v_g(-k)]/2$ and $\Delta\tilde{A}_{\mathrm{STT}} = [\Delta\tilde{A}(k) - \Delta\tilde{A}(-k)]/2$. For a fixed j direction, only the intrinsic effect of STT changes its sense with respect to the inversion of wave vector k, while the effects of the Oersted field, Joule heating, and so on do not. The Δv_{STT} and $\Delta\tilde{A}_{\mathrm{STT}}$ can cancel out the latter effects and increase the evaluation accuracy. Here, note that we used the normalized amplitude due to the nonreciprocity of the MSSW [25]. The time shift values were obtained by calculating the cross correlation of two different SW waveforms.

Figure 2(a) shows the result of the SW Doppler shift detected in the real-time measurement for the device with $x = 20$ μm, where the Δv_{STT} obtained by averaging over 20 independent measurements is plotted as a function of injection current j. For instance, the SW packet in a "downstream" condition with the negative j is accelerated to yield $\Delta v_{\mathrm{STT}} \sim 4$ m/s at $j = -0.8 \times 10^{11}$ A/m^2 injection, while the SW packet in an "upstream" one ($j > 0$) is decelerated, resulting in $\Delta v_{\mathrm{STT}} \sim -4$ m/s at $j = 0.8 \times 10^{11}$A/m^2. Thus, the Δv_{STT} is linearly dependent on j. According to Eq. (1), the slope of $\Delta v_{\mathrm{STT}}/j$ gives the spin polarization $P = 0.60 \pm 0.03$.

The spin polarizations P deduced from the devices with different gap sizes are compiled in Fig. 2(b). The devices with $x = 20$, 25, and 30 μm provide a consistent estimation of spin polarization $\langle P\rangle = 0.60 \pm 0.02$. Although the results for the devices with $x = 10$ and 40 μm give similar values, they have large error bars, because the time resolution limits the evaluation of v_{STT} in the 5 μm case and the attenuated SW shape makes it difficult to precisely determine Δv_{STT} in the 40 μm case [for example, see Fig. 1(b)]. Nevertheless, the obtained polarization is in good agreement with the frequency domain result $P = 0.60 \pm 0.02$ [18], which verifies that our time-domain measurement possesses a sufficient resolution to detect the STT-induced SW Doppler shift.

Figure 2(c) represents the SW attenuation due to the current injection for the device with $x = 20$ μm; the SW packet is amplified by 0.2% for the downstream current $j = -0.8 \times 10^{11}$ A/m^2 injection, while it is attenuated by 0.2% in the upstream current $j = 0.8 \times 10^{11}$ A/m^2. The j dependence of $\Delta\tilde{A}_{\mathrm{STT}}$ shows a linear slope, from which the nonadiabatic STT is deduced to be $\beta = 0.02 \pm 0.013$ by using Eq. (3). Note that the change in SW amplitude is less than 0.2%, so one can consider $\ln(\tilde{A}_{\mathrm{STT}}) \cong \Delta\tilde{A}_{\mathrm{STT}}$. The magnitudes of β for different devices are deduced by using simultaneously determined P and plotted in Fig. 2(d), although the change of SW amplitude is not sufficiently large to precisely evaluate for $x = 40$ μm. Importantly, the magnitude of β for the different devices falls in the same range for the devices with different gap sizes, yielding $\langle\beta\rangle = 0.033 \pm 0.012$. The present result implies $\beta \sim 4\alpha$.

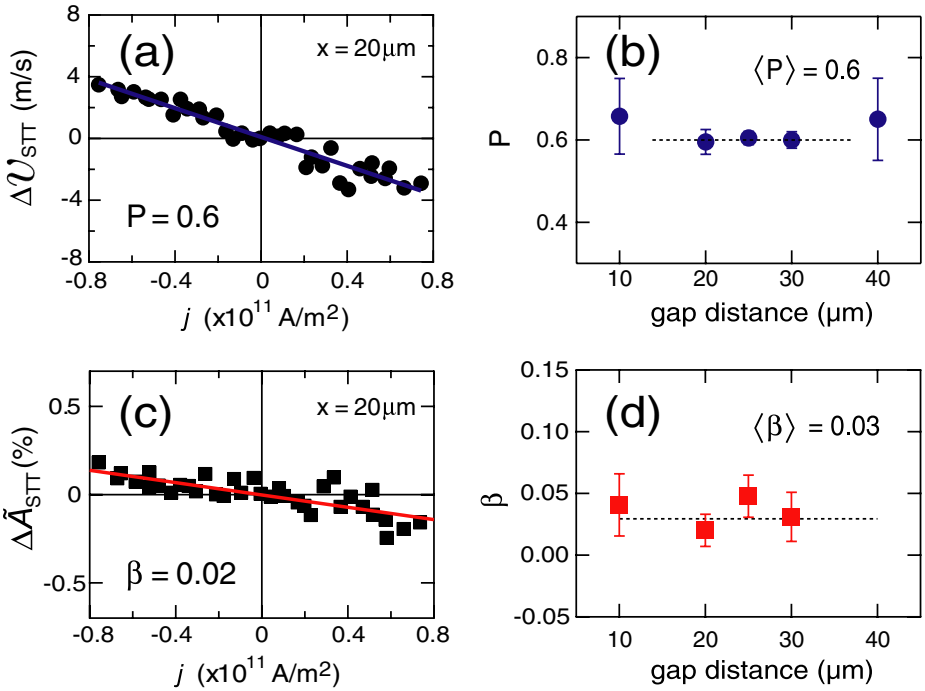

FIG. 2 (color online). Experimental data of the current-induced modulations. (a) The spin wave Doppler shift induced by electric current ($x = 20$ μm). (b) Spin polarization P measured for several devices with different gap distances. (c) The spin wave attenuation induced by electric current ($x = 20$ μm). (d) Nonadiabaticity of STT (β) deduced from the attenuation of SW amplitude.

To check the validity of the method used in the experimental analysis, we performed the micromagnetic simulation. We used the modified Landau-Lifshitz-Gilbert equation with spin torque terms describing the time-dependent magnetization dynamics. From the simulated SW mode similar with the time-domain signal in Fig. 2(b), we evaluated the time delay (Ref. [21]) and SW attenuation depending on the bias current. Figure 3(a) shows the bias current-dependent SW attenuation where the current-induced Oersted field was not considered (denoted by "without H_{Oe}"). $\Delta\tilde{A}_{STT}$ linearly depends on the bias current and the detection position. But, as shown in Fig. 3(b), such a linear dependence cannot be observed when the Oersted field is considered. Such a nonlinear behavior is due to the fact that the Oersted field is spatially distributed inside the film. To exclude the Oersted field effect, we calculate $\Delta\tilde{A}_{STT} = [\Delta\tilde{A}(k) - \Delta\tilde{A}(-k)]/2$ [as denoted by the open symbols in Fig. 3(c)] as the subtraction procedure used in the experiment. Compared to $\Delta\tilde{A}$ without the Oersted field [as denoted by the solid symbols in Fig. 3(c)], the linear bias dependence is similar; however, there is a quantitative difference that indicates that the Oersted field effect is not completely excluded. Figure 3(d) shows the β (fitting) evaluated value by using Eq. (3) with the slope of Fig. 3(c) as a function of β (input) considered in the modified Landau-Lifshitz-Gilbert equation. The black line represents the reference line corresponding to "β(input) = β(fitting)." The red square represents β (fitting) in the presence of the Oersted field, and the red line corresponds to its linear fit. The error bars were obtained from the statistical analysis of deduced β in the range of $x = 20$–50 μm and $j = -0.7$– $+ 0.7(\times 10^{11}$ A/m$^2)$. The β (fitting) is somewhat different from the β (input). Also, as shown in the inset, the difference linearly increases with β. We attributed this inaccuracy to the slightly noncollinear magnetization profile along the thickness direction of the film owing to the spatially distributed Oersted field. We found from the modeling study that the Oersted field effect on the beta estimation becomes negligible when $t_{Py} < 15$ nm (not shown).

Experimentally, $\langle\beta\rangle = 0.033 \pm 0.012$; however, the careful micromagnetic modeling proves that the Oersted field effect causes an overestimation of β. According to the modeling results, $\beta = 0.03$ corresponds to $\beta = 0.02$, so that the experimental value of β falls into the range 2α–3α.

Next, we discuss the physical meaning of our results. First, as mentioned above, we used nonlocal magnetization texture (= MSSW) so that our approach would give a more correct estimation of β than experiments performed for a local object (= DW) that is sensitive to local defects. Second, there are two mechanisms contributing to nonzero β: the spin relaxation [20] and the ballistic spin mistrack [26]. The β term caused by the former is constant regardless of the spatial gradient of magnetization (i.e., DW width), whereas that caused by the latter becomes significant as the DW width gets smaller than the characteristic length scale of the spin density precession. Since the

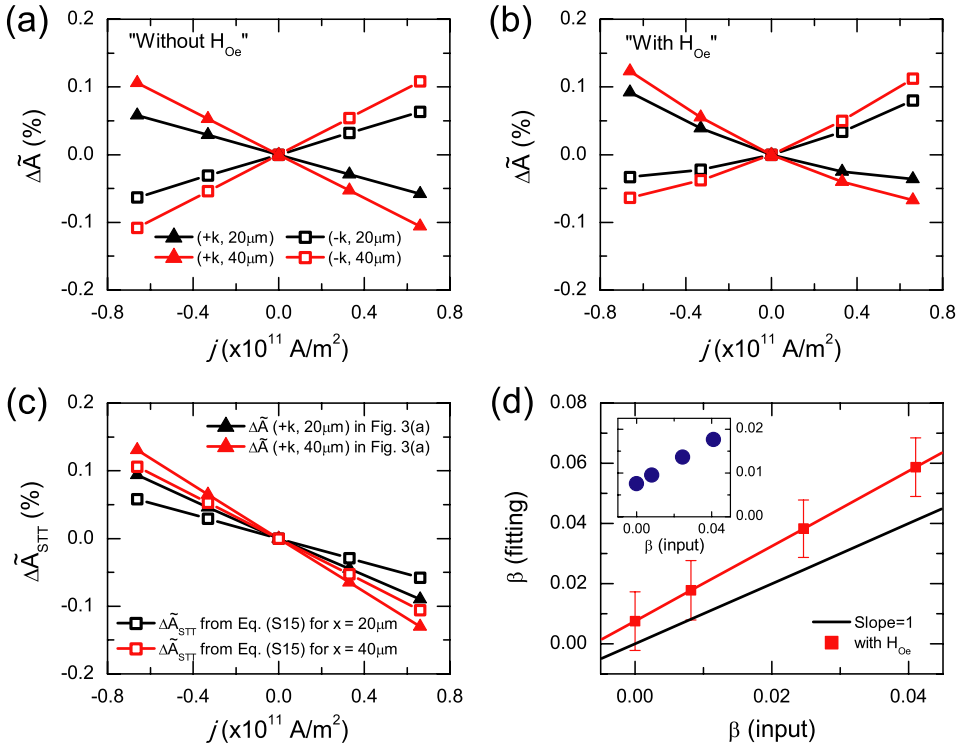

FIG. 3 (color online). Current-induced modulation of the SW amplitude and the nonadiabaticity β (micromagnetic simulation). (a) Current-induced modulation of the SW amplitude in the absence of the Oersted field effect ($\beta = 3\alpha$). (b) Current-induced modulation of the SW amplitude in the presence of the Oersted field effect ($\beta = 3\alpha$). The solid triangles and open squares represent the case of forward propagating SWs ($+ k$) and backward propagating SWs ($- k$), respectively. The black and red symbols represent the case of the detection position $x = 20$ and 40 μm, respectively. (c) Comparison of the current-induced modulation of the SW amplitude evaluated from the subtraction method as Eq. (S15) ($\Delta\tilde{A}_{\mathrm{STT}}$, open triangles) and that estimated in the absence of the Oersted field ($\tilde{A}$, solid squares) ($\beta = 3\alpha$). (d) β (input) vs β (fitting). The red symbols correspond to the case in the presence of the Oersted field effect, and the solid line corresponds to slope $= 1$ meaning β(input) $= \beta$(fitting). The inset shows the difference of β (input) and β (fitting).

spatial gradient of MSSW is much smaller than that of a typical DW, we are able to exclude the contribution of the ballistic spin mistrack. Thus, our result ($\beta = 2\alpha$ to 3α) indicates that the β term caused by the spin relaxation is of the order of the damping constant, consistent with theories [27].

The present approach of real-time monitoring of the SW propagation has a clear advantage in that several subtle effects such as the Joule heating and edge roughness of devices are presumably less serious than in the DW experiments. Another advantage of the present time-domain experiments of propagating spin wave spectroscopy lies in that we can simultaneously determine P, α, and β in a single series of experiments. As the SW is inherent in every magnetic system, this method would give a value of β for any magnetic material, even if the DW motion would not be electrically induced. By improving the resolution of propagating spin wave spectroscopy to determine SW amplitude, it could serve as a standard tool to estimate the above three parameters governing the STT physics. A systematic study for different materials to compile these parameters could help to elucidate the microscopic origin of spin transfer dynamics and to explore new efficient spintronic devices and techniques, such as the SW amplification in materials with appropriate P, α, and β.

We acknowledge Dr. R. D. McMichael and Dr. V. Vlaminck for fruitful discussions. This work was supported in part by Grant-in-Aid for Creative Scientific Research from MEXT and Grant-in-Aid for Scientific Research(S) from JSPS. K.-J. L. acknowledges support from NRF/MEST (Contract No. 2010-0023798).

[1] S. A. Wolf *et al.*, Science **294**, 1488 (2001).
[2] A. Ney, C. Pampuch, R. Koch, and K. H. Ploog, Nature (London) **425**, 485 (2003).
[3] J. S. Moodera and P. LeClair, Nature Mater. **2**, 707 (2003).
[4] S. S. P. Parkin *et al.*, J. Appl. Phys. **85**, 5828 (1999).
[5] C. Chappert, A. Fert, and F. N. Van Dau, Nature Mater. **6**, 813 (2007).
[6] A. Thiaville, Y. Nakatani, J. Miltat, and Y. Suzuki, Europhys. Lett. **69**, 990 (2005).

[7] S. S. P. Parkin, M. Hayashi, and L. Thomas, Science **320**, 190 (2008).
[8] M. Tsoi *et al.*, Phys. Rev. Lett. **80**, 4281 (1998).
[9] E. B. Myers *et al.*, Science **285**, 867 (1999).
[10] M. Tsoi *et al.*, Nature (London) **406**, 46 (2000).
[11] A. Yamaguchi *et al.*, Phys. Rev. Lett. **92**, 077205 (2004).
[12] L. Thomas *et al.*, Nature (London) **443**, 197 (2006).
[13] M. Hayashi *et al.*, Phys. Rev. Lett. **96**, 197207 (2006).
[14] R. Moriya *et al.*, Nature Phys. **4**, 368 (2008).
[15] L. Heyne *et al.*, Phys. Rev. Lett. **100**, 066603 (2008).
[16] P. Lederer and D. L. Mills, Phys. Rev. **148**, 542 (1966).
[17] V. Vlaminck and M. Bailleul, Science **322**, 410 (2008).
[18] M. Zhu, C. L. Dennis, and R. D. McMichael, Phys. Rev. B **81**, 140407 (2010).
[19] S. M. Seo, K. J. Lee, H. Yang, and T. Ono, Phys. Rev. Lett. **102**, 147202 (2009).
[20] S. Zhang and Z. Li, Phys. Rev. Lett. **93**, 127204 (2004).
[21] See Supplemental Material at http://link.aps.org/supplemental/10.1103/PhysRevLett.108.017203 for the derivation of formulas.
[22] M. Covington, T. M. Crawford, and G. J. Parker, Phys. Rev. Lett. **89**, 237202 (2002).
[23] D. D. Stancil, *Theory of Magnetostatic Waves* (Springer-Verlag, New York, 1993).
[24] M. Bailleul, D. Olligs, C. Fermon, and S. O. Demokritov, Europhys. Lett. **56**, 741 (2001).
[25] K. Sekiguchi *et al.*, Appl. Phys. Lett. **97**, 022508 (2010).
[26] G. Tatara and H. Kohno, Phys. Rev. Lett. **92**, 086601 (2004); G. Tatara *et al.*, J. Phys. Soc. Jpn. **76**, 054707 (2007); J. Xiao, A. Zangwill, and M. D. Stiles, Phys. Rev. B **73**, 054428 (2006).
[27] Y. Tserkovnyak, A. Brataas, and G. E. W. Bauer, J. Magn. Magn. Mater. **320**, 1282 (2008).